








Article

Neuro-Axonal Damage and Alteration of Blood–Brain Barrier Integrity in COVID-19 Patients

Maria Antonella Zingaropoli ^{1,*}, Marco Iannetta ², Lorenzo Piermatteo ³, Patrizia Pasculli ¹, Tiziana Latronico ⁴, Laura Mazzuti ^{5,6}, Laura Campogiani ², Leonardo Duca ³, Giampiero Ferraguti ⁷, Manuela De Michele ⁸, Gioacchino Galardo ⁹, Francesco Pugliese ¹⁰, Guido Antonelli ⁵, Massimo Andreoni ², Loredana Sarmati ², Miriam Lichtner ^{1,11}, Ombretta Turriziani ⁵, Francesca Ceccherini-Silberstein ³, Grazia Maria Liuzzi ⁴, Claudio Maria Mastroianni ¹ and Maria Rosa Ciardi ¹

- ¹ Department of Public Health and Infectious Diseases, Sapienza University of Rome, 00185 Rome, Italy
 - ² Department of Systems Medicine, Tor Vergata University of Rome, 00133 Rome, Italy
 - ³ Department of Experimental Medicine, Tor Vergata University of Rome, 00133 Rome, Italy
 - ⁴ Department of Biosciences, Biotechnologies and Biopharmaceutics, University of Bari Aldo Moro, 70126 Bari, Italy
 - ⁵ Department of Molecular Medicine, Sapienza University of Rome, 00161 Rome, Italy
 - ⁶ Department of Clinical and Molecular Medicine, Sapienza University of Rome, 00161 Rome, Italy
 - ⁷ Department of Experimental Medicine, Sapienza University of Rome, 00161 Rome, Italy
 - ⁸ Emergency Department Stroke Unit, Department of Human Neurosciences, Sapienza University of Rome, 00161 Roma, Italy
 - ⁹ Medical Emergency Unit, Sapienza University of Rome, Policlinico Umberto I, 00161 Rome, Italy
 - ¹⁰ Department of Specialist Surgery and Organ Transplantation “Paride Stefanini”, Policlinico Umberto I, Sapienza University of Rome, 00161 Rome, Italy
 - ¹¹ Infectious Diseases Unit, SM Goretti Hospital, Sapienza University of Rome, 04100 Latina, Italy
- * Correspondence: mariaantonella.zingaropoli@uniroma1.it; Tel.: +39-0649970607



Citation: Zingaropoli, M.A.; Iannetta, M.; Piermatteo, L.; Pasculli, P.;

Latronico, T.; Mazzuti, L.; Campogiani, L.; Duca, L.; Ferraguti, G.; De Michele, M.; et al. Neuro-Axonal Damage and Alteration of Blood–Brain Barrier Integrity in COVID-19 Patients. *Cells* **2022**, *11*, 2480. <https://doi.org/10.3390/cells11162480>

Academic Editors: Christian Barbato, Antonio Minni and Carla Petrella

Received: 6 July 2022

Accepted: 7 August 2022

Published: 10 August 2022

Publisher’s Note: MDPI stays neutral with regard to jurisdictional claims in published maps and institutional affiliations.



Copyright: © 2022 by the authors. Licensee MDPI, Basel, Switzerland. This article is an open access article distributed under the terms and conditions of the Creative Commons Attribution (CC BY) license (<https://creativecommons.org/licenses/by/4.0/>).

Abstract: Neurofilament light chain (NfL) is a specific biomarker of neuro-axonal damage. Matrix metalloproteinases (MMPs) are zinc-dependent enzymes involved in blood–brain barrier (BBB) integrity. We explored neuro-axonal damage, alteration of BBB integrity and SARS-CoV-2 RNA presence in COVID-19 patients with severe neurological symptoms (neuro-COVID) as well as neuro-axonal damage in COVID-19 patients without severe neurological symptoms according to disease severity and after recovery, comparing the obtained findings with healthy donors (HD). Overall, COVID-19 patients ($n = 55$) showed higher plasma NfL levels compared to HD ($n = 31$) ($p < 0.0001$), especially those who developed ARDS ($n = 28$) ($p = 0.0005$). After recovery, plasma NfL levels were still higher in ARDS patients compared to HD ($p = 0.0037$). In neuro-COVID patients ($n = 12$), higher CSF and plasma NfL, and CSF MMP-2 levels in ARDS than non-ARDS group were observed ($p = 0.0357$, $p = 0.0346$ and $p = 0.0303$, respectively). SARS-CoV-2 RNA was detected in four CSF and two plasma samples. SARS-CoV-2 RNA detection was not associated to increased CSF NfL and MMP levels. During COVID-19, ARDS could be associated to CNS damage and alteration of BBB integrity in the absence of SARS-CoV-2 RNA detection in CSF or blood. CNS damage was still detectable after discharge in blood of COVID-19 patients who developed ARDS during hospitalization.

Keywords: neurofilament light chain; NfL; matrix metalloproteinases; MMPs; ddPCR; long-COVID; neuro-COVID; zymography

1. Introduction

The severe acute respiratory syndrome coronavirus 2 (SARS-CoV-2), which causes the coronavirus disease 2019 (COVID-19), has infected more than five hundred million people and has caused more than six million deaths globally, as of 5 July 2022 (available online: <https://covid19.who.int>, accessed on 5 July 2022). Whereas SARS-CoV-2 is known to cause mainly pulmonary diseases, including pneumonia and acute respiratory distress syndrome

(ARDS), clinicians have observed many extrapulmonary manifestations of COVID-19 [1]. The emerging literature suggests that the hematologic, cardiovascular, renal, gastrointestinal, and hepatobiliary, endocrinologic, neurologic, ophthalmologic, and dermatologic systems can all be affected [2–6]. Several non-specific mild neurological symptoms can be observed in patients with COVID-19, including headache, anorexia, myalgia, fatigue, dizziness, anosmia, and ageusia [2,7,8], with variable incidence if we consider outpatients with milder presentations or inpatients with more severe disease forms [7,9,10]. In severe neurological cases of COVID-19, cerebrovascular accidents [11,12], confusion and impaired consciousness [13,14] can represent the clinical presentation of the disease. Acute inflammatory demyelinating polyneuropathy has also been reported in some patients [15,16]. In addition, meningoencephalitis [17], hemorrhagic posterior reversible encephalopathy syndrome [18], and acute necrotizing encephalopathy, involving the brainstem and basal ganglia, have been described in case reports [19,20]. Ocular manifestations, such as conjunctival congestion alone, conjunctivitis, and retinal changes, have also been reported in patients with COVID-19 [7,21–23].

SARS-CoV-2 RNA detection in the cerebrospinal fluid (CSF) represents the evidence of the ability of this virus to invade the central nervous system (CNS), although viral isolation in cellular culture represents the definitive sign of SARS-CoV-2 productive neuroinvasion [24]. In May 2020, Moriguchi and colleagues [19] were the first to report the presence of SARS-CoV-2 RNA in the CNS, using a real-time reverse transcription-polymerase chain reaction (RT-PCR) on a CSF sample of a patient with COVID-19 associated encephalopathy. Further cases have since been reported [25–27]. However, SARS-CoV-2 RNA was inconstantly detected in the CSF of COVID-19 patients with neurological manifestations [17,28,29].

In the management of neurological diseases, the identification and quantification of axonal damage can improve the diagnostic accuracy and prognostic assessment. Neurofilaments (Nf) are major components of the neuronal cytoskeleton, consisting predominantly of three subunits: Nf-light (NfL), Nf-medium, and Nf-heavy chains. Each subunit possesses a particular molecular mass, and their relative concentration is uneven. Upon neuro-axonal damage, NfL, the most abundant and soluble of the subunits [30], is released into the extracellular space and is detectable in the CSF and blood [31]. Its levels increase in CSF and blood proportionally to the degree of axonal damage in a variety of neurological disorders, including inflammatory, neurodegenerative, traumatic, cerebrovascular diseases, and in prion associated encephalopathy [32–34]. Evidence that both CSF and blood NfL may serve as diagnostic, prognostic, and monitoring biomarkers in neurological diseases are progressively accumulating, and NfL is one of the most promising biomarkers to be used in clinical and research settings in the near future [35].

Matrix metalloproteinases (MMPs) are zinc-dependent enzymes that degrade extracellular matrix (ECM) proteins, such as collagen, fibronectin, and laminin as well as basal membrane structures. MMPs are mediators of neuroinflammatory processes, by regulating blood–brain barrier (BBB) integrity, neutrophil infiltration in the CNS, and cytokine signaling [36]. The involvement of MMPs in the impairment of BBB integrity during viral infections of the CNS has been extensively reviewed elsewhere [37]. Clinical evidence from patients with viral meningitis have demonstrated elevated CSF levels of MMP-9 and tissue inhibitor of matrix metalloproteinases-1 (TIMP-1) compared to control patients [38]. Moreover, increased levels of chemokines, MMPs, and TIMP-1 have been reported in the CSF of patients with Varicella-zoster virus (VZV) infection and HIV infection [39,40], and in mice with lethal infection with neurotropic mouse hepatitis virus [41].

The primary aim of this study was to explore CSF and plasma NfL levels as well as CSF MMP-2 and MMP-9 levels in COVID-19 patients with severe neurological symptoms. The secondary aim was to evaluate in a cross-sectional and longitudinal approach plasma NfL levels in COVID-19 patients stratified according to disease severity during the acute phase of the disease and after recovery.

2. Materials and Methods

2.1. Patients and Clinical Samples Collection

Hospitalized COVID-19 patients were enrolled. COVID-19 related pneumonia was diagnosed by chest computed tomography (CT scan) associated with SARS-CoV-2 RNA detection on a nasopharyngeal swab, as previously described [6,42]. For all enrolled COVID-19 patients, whole blood samples were collected in heparin tubes during routine clinical testing on hospital admission (baseline) and after three months from hospital discharge (Tpost) (Figure 1A).

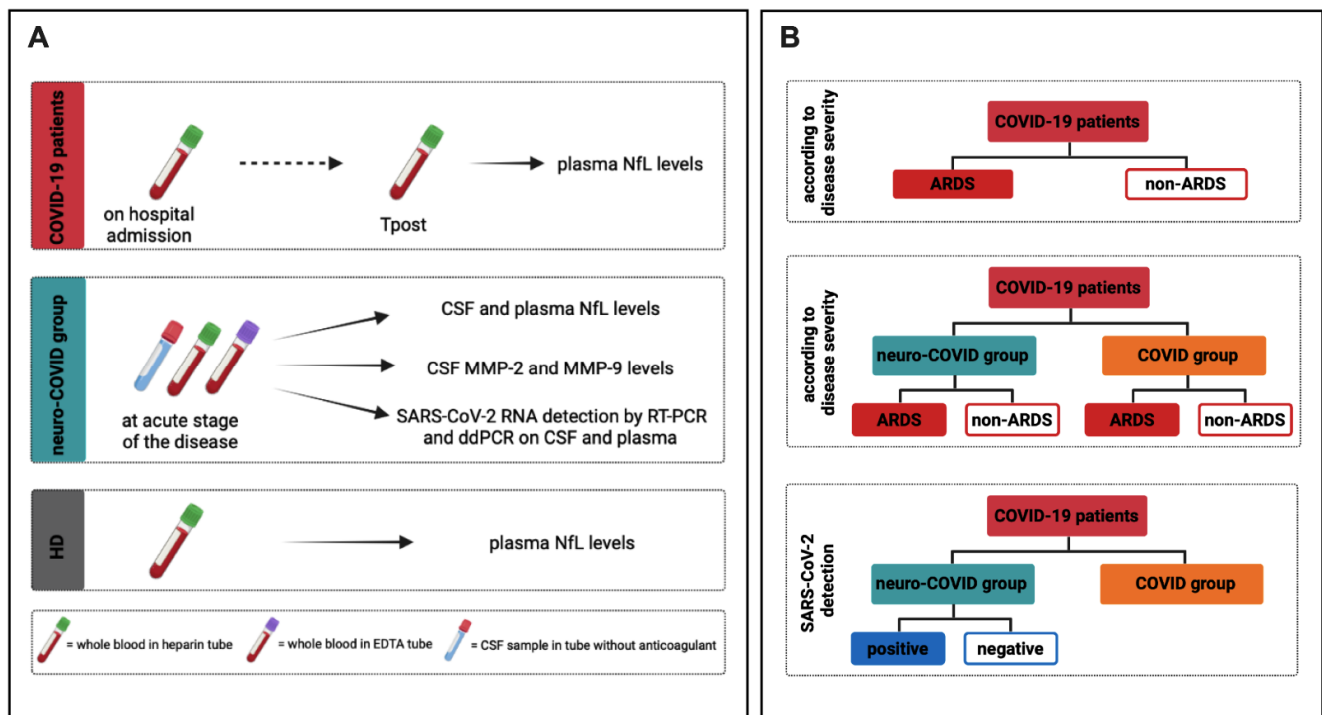


Figure 1. Study design. (A) For COVID-19 patients, whole blood samples were collected in heparin tubes during routine clinical testing at two timepoints: on hospital admission (baseline) and after three months from discharge (Tpost). For the neuro-COVID group, CSF samples and heparin and EDTA whole blood samples were collected. RT-PCR and ddPCR were used for the detection and quantification of SARS-CoV-2 RNA in collected CSF and whole blood samples. For healthy donors (HD) heparin whole blood samples were collected. (B) According to clinical outcome, COVID-19 patients were stratified into ARDS and non-ARDS groups and the differences in plasma NfL levels were evaluated. According to disease severity, both neuro-COVID group and COVID groups were stratified into ARDS and non-ARDS groups and the differences in CSF NfL levels, plasma NfL levels, and CSF MMP-2 and MMP-9 levels were assessed. According to the detection of SARS-CoV-2 RNA in CSF and plasma samples, neuro-COVID group was stratified into positive and negative groups and the differences in CSF NfL levels as well as MMP-2 and MMP-9 levels were evaluated. Neuro-COVID group: COVID-19 patients with severe neurological symptoms; COVID group: COVID-19 patients without severe neurological symptoms; NfL: neurofilament light chain; MMP-2: matrix metalloprotease-2; MMP-9: matrix metalloprotease-9; SARS-CoV-2: severe acute syndrome coronavirus 2; RT-PCR: reverse transcription-polymerase chain reaction; ddPCR: droplet digital polymerase chain reaction; CSF: cerebrospinal fluid; HD: healthy donors; EDTA: ethylenediaminetetraacetic acid; ARDS: acute respiratory distress syndrome.

Patients were stratified according to the occurrence of severe neurological symptoms into two groups: with (neuro-COVID group) and without (COVID group) severe neurological symptoms. For the neuro-COVID group, CSF samples were collected in sterile tubes without anticoagulant whereas whole blood samples were collected in heparin and

ethylenediaminetetraacetic acid (EDTA) tubes. Samples were drawn at the acute phase of the disease, during routine clinical testing (Figure 1A). Finally, healthy donors (HD) age and sex matched with COVID-19 patients, with negative nasopharyngeal swab for SARS-CoV-2 RNA detection and undetectable anti-SARS-CoV-2 Nucleoprotein (N) specific IgG on the sampling day, were enrolled (Figure 1A). Heparin and EDTA plasma samples were obtained after centrifugation and immediately stored at $-80\text{ }^{\circ}\text{C}$ until use. CSF samples were stored at $-80\text{ }^{\circ}\text{C}$ until use.

As reported in Figure 1B, COVID-19 patients were stratified according to disease severity into ARDS and non-ARDS groups. ARDS was defined according to the 2012 Berlin criteria [43]. Both neuro-COVID and COVID groups were further stratified according to disease severity (Figure 1B). Finally, neuro-COVID group was stratified based on the detection of SARS-CoV-2 RNA in CSF and plasma samples (Figure 1B), and the differences in CSF NfL levels as well as MMP-2 and MMP-9 activity were evaluated.

Finally, COVID-19 patients were further stratified into four groups according to the maximal oxygen supply/ventilation support required during the hospitalization: ambient air (AA), Venturi oxygen mask (VMK), noninvasive ventilation (NIV), and invasive mechanical ventilation through orotracheal intubation (IOT), and the differences in plasma NfL levels were evaluated.

2.2. Evaluation of CSF and Plasma NfL Levels in Collected Samples

As previously described [44], the evaluation of NfL levels in collected samples were assessed using the Simple Plex™ Ella Assay (ProteinSimple, San Jose, CA, USA) on Ella™ microfluidic system (Bio-Techne, Minneapolis, MN, USA) according to the manufacturers' instructions. Ella™ was calibrated using the in-cartridge factory standard curve. The limit of detection of NfL was 1.09 pg/mL , calculated by adding three standard deviations to the mean background signal determined from multiple runs.

2.3. Evaluation of Gelatinase Activity by Zymography

For the neuro-COVID group, the evaluation of CSF MMP-2 and MMP-9 levels was performed by SDS-PAGE zymography as previously described [40,45]. Briefly, $50\text{ }\mu\text{L}$ of each CSF sample were precipitated for 1 h at $-20\text{ }^{\circ}\text{C}$ in cold acetone, then the samples were centrifuged, and the pellets solubilized in $10\text{ }\mu\text{L}$ of loading buffer containing SDS. Samples were then applied on 10% polyacrylamide gels ($10\text{ cm} \times 10\text{ cm}$), which had been copolymerized with 0.1% (*w/v*) gelatin. Stacking gels contained 5.4% polyacrylamide. Electrophoresis was carried out at $4\text{ }^{\circ}\text{C}$ for approximately 2 h at 100 V. After electrophoresis, the gels were washed for $2 \times 30\text{ min}$ in 2.5% (*w/v*) Triton X-100 in 100 mM Tris-HCl, pH 7.4 (washing buffer) to remove SDS and reactivate the enzyme, then incubated for 24 h at room temperature in 100 mM Tris-HCl, pH 7.4 (developing buffer).

For the development of the enzyme activity, the substrate in the gels was stained with Coomassie brilliant blue R-250 and destained in methanol/acetic acid/ H_2O . Gelatinase activity was detected as a white band on a blue background and was quantified by computerized image analysis through two-dimensional scanning densitometry.

2.4. SARS-CoV-2 RNA Evaluation in CSF and Plasma Samples

For the neuro-COVID group, real-time RT-PCR and digital droplet PCR (ddPCR) were used for the detection and quantification of SARS-CoV-2 RNA in collected samples.

For real-time RT-PCR, total RNA was extracted from 1.5 mL of CSF and plasma using the Total Purification RNA kit (Norgen Biotek Corp., Thorold, ON, Canada) after virus concentration by centrifugation at higher speed, as previously described [46].

For SARS-CoV-2 RNA quantification by ddPCR, total RNA was extracted from $280\text{ }\mu\text{L}$ of samples using the QIAamp viral RNA mini kit (Qiagen, Hilden, Germany) according to manufacturer's instruction and concentrated up to $10\text{ }\mu\text{L}$ by using Savant DNA SpeedVac (Thermo Fisher Scientific, Waltham, MA, USA). SARS-CoV-2 RNA was quantified by QX200™ Droplet Digital™ PCR System (ddPCR, Biorad, Hercules, CA, USA) using an

in-house assay, targeting the RdRP gene of SARS-CoV-2 as previously described [47,48]. The assay also targets the housekeeping gene RNase P as internal control of amplification. The ddPCR assay provides an absolute quantification of viral RNA without a calibration curve and the results were expressed as copies/mL. Despite the standard curve, it is not necessary for proper DNA/RNA quantification; thus, the use of controls is very important, especially to better discriminate false positivity. As previously reported [47], our ddPCR assay for SARS-CoV-2 RNA quantification also shows a good linearity and reproducibility for the detection of a single RNA copy for reaction. At least 4 negative controls every 24 quantifications were used. The negative controls are treated as samples, starting from the extraction until the quantification, to exclude any potential contamination or procedure bias.

2.5. Statistical Analysis

All statistical analyses were performed using GraphPad Prism v.9 software and two-tailed $p \leq 0.05$ was considered statistically significant. Values are represented as median and interquartile range (IQR). The nonparametric comparative Mann–Whitney test was used for comparing medians between COVID-19 patients and HD as well as between neuro-COVID and COVID groups and between ARDS and non-ARDS groups. The nonparametric comparative Wilcoxon test was used for longitudinal evaluation between biomarkers assessed at baseline and Tpost in the COVID group. Spearman rank correlation analysis was used to assess the relation between CSF and plasma NfL levels.

3. Results

3.1. Clinical and Demographical Feature of Study Population

Fifty-five hospitalized COVID-19 patients and 31 HD were enrolled (Table 1). According to chest CT scan, all COVID-19 patients had interstitial pneumonia and 52.7% had ARDS. Overall, 12.7% of COVID-19 patients died, and 21.8% of COVID-19 patients showed severe neurological symptoms (neuro-COVID group) (Table 1).

Table 1. Demographic and clinical features in COVID-19 patients.

	COVID-19 Patients (n = 55)	HD (n = 31)	p Value *
Male/Female	32/23	15/16	ns
Age, years	63 (55–73)	64 (55–70)	ns
ARDS/non-ARDS	26/29	-	-
Deaths/Alive	7/48	-	-
Comorbidities			
Any	32	-	-
Hypertension	19	-	-
Cardiovascular	4	-	-
Diabetes	6	-	-
Pulmonary	4	-	-
Cancer	6	-	-
Renal	1	-	-
Symptoms			
Fever	44	-	-
Cough	26	-	-
Shortness of breath	19	-	-
Myalgia or arthralgia	14	-	-
Neurological symptoms	12	-	-
Diarrhea	7	-	-
Anosmia and ageusia	4	-	-
Sputum production	1	-	-
Laboratory finding			
WBC ($\times 10^9/L$)	4.9 (4.2–5.8)	-	-
Neutrophils ($\times 10^9/L$)	3.5 (2.3–4.1)	-	-
Lymphocytes ($\times 10^9/L$)	1.1 (0.7–1.5)	-	-

Table 1. *Cont.*

	COVID-19 Patients (<i>n</i> = 55)	HD (<i>n</i> = 31)	<i>p</i> Value *
NLR	2.9 (1.6–5.2)	-	-
CRP (mg/dL)	3.4 (1.3–11.7)	-	-
D-dimer (µg/mL)	823 (443–1702)	-	-
Ferritin (ng/mL)	493 (264–1445)	-	-
LDH (U/L)	260 (201–354)	-	-
P/F ratio	343 (293–407)	-	-

HD: healthy donors, *n*: number, ARDS: acute respiratory distress syndrome, WBC: white blood cells, NLR: neutrophil/lymphocyte ratio, CRP: C-reactive protein, LDH: lactate dehydrogenase, P/F: arterial oxygen partial pressure/fraction of inspired oxygen. Data are shown as median (interquartile range). * The 2-tailed X2 test or Fisher's exact test and the nonparametric comparative Mann–Whitney test were used for comparing proportions and medians, respectively, between COVID-19 patients and HD.

As reported in Table 2, in neuro-COVID group the most frequent neurological signs and symptoms included confusion and headache. Among less common symptoms, we observed a case of gaze deviation to the right, nystagmus, seizures, forced deviation of the head to the left, and bilateral vision impairment. Finally, a stroke, a meningoencephalitis and a bilateral optic neuritis were observed (Table 2). A CSF laboratory examination was reported in Table 3.

Table 2. Demographic and clinical features of neuro-COVID group.

Patient	Gender	Age	Comorbidities	Neurologic Signs and Symptoms	Real-Time RT-PCR in Nasopharyngeal Swab (Ct Values)	Neurological Outcomes	Outcome
1	♂	67	-	confusion	positive (20.4)		discharged
2	♂	83	diabetes mellitus (type II) arterial	confusion, syncope	positive (30.9)		discharged
3	♀	70	hypertension and chronic lymphoid leukemia	headache, confusion	positive (29.5)		discharged
4	♀	61	dyslipidemia	nystagmus, seizure, forced deviation of the head to the left	positive (n.a.)		discharged
5	♂	86	diabetes mellitus (type II), dyslipidemia, arterial hypertension	weakness, headache, gaze deviation to the right	positive (n.a.)	stroke	discharged
6	♀	58	bronchial asthma	headache, confusion	positive (24.7)		discharged
7	♂	36	acute myeloid leukemia	headache, confusion	positive (10.4)	meningoencephalitis	death
8	♂	69	-	lower limb paresthesia	positive (14.0)		discharged
9	♀	67	bronchial asthma, arterial hypertension, right nephrectomy, anemia	headache, confusion	positive (15.7)		discharged
10	♀	62	diabetes mellitus (type II), dyslipidemia, arterial hypertension	impaired bilateral vision and frontal headache	positive (32.3)	bilateral optic neuritis	discharged

Table 2. Cont. .

Patient	Gender	Age	Comorbidities	Neurologic Signs and Symptoms	Real-Time RT-PCR in Nasopharyngeal Swab (Ct Values)	Neurological Outcomes	Outcome
11	♂	78	arterial hypertension, diabetes mellitus (type II)	headache, confusion	positive (28.8)		death
12	♀	60	solid tumor	headache, confusion	positive (24.1)		discharged

RT-PCR: reverse transcription-polymerase chain; Ct: cycle threshold; n.a.: not available.

Table 3. CSF examination of neuro-COVID group.

Patient	Appearance	Protein mg/dL [15–45]	Glucose mg/dL [50–80]	Albumin mg/dL [0–35]	Lactic Acid mmol/L [1.1–2.4]	Cell Count/ μ L [<10]	QAlb [0–9]	Real-Time RT-PCR in CSF (Ct Values)	Real-Time RT-PCR in Plasma	ddPCR in CSF (RdRp cp/mL)	ddPCR in Plasma (RdRp cp/mL)
1	clear	28	80	8.2	1.1	2	3.3	negative	negative	negative	negative
2	clear	34	104	9.1	2.1	1	4.3	negative	negative	negative	negative
3	clear	17.2	76	9.3	1.4	1	2.6	negative	negative	positive (11.0)	negative
4	clear	18.2	89	8.9	1.6	1	3.1	negative	negative	negative	negative
5	clear	28.9	98	8.3	3.2	2	2.5	negative	negative	negative	negative
6	clear	37.0	64	9.1	3.4	5	4.0	negative	negative	negative	negative
7	clear	19.6	61	10.5	3.3	16	3.6	negative	negative	positive (8.1)	negative
8	clear	39.6	56	20.9	3.3	3	6.1	negative	negative	negative	positive (2.0)
9	clear	55.8	101	35.9	3.4	4	9.4	negative	negative	positive (2.0)	negative
10	clear	29.4	151	17.9	3.1	5	5.0	negative	negative	negative	negative
11	clear	25.0	71	10.0	2.3	1	4.3	negative	negative	negative	positive (14.0)
12	clear	47.0	86	29.9	1.8	5	7.4	positive (34.3)	negative	positive (14.0)	negative

QAlb: CSF/serum albumin quotient; RT-PCR: reverse transcription-polymerase chain reaction; Ct: cycle threshold, ddPCR: droplet digital polymerase chain reaction; RdRp: RNA-dependent RNA polymerase; cp: copy.

3.2. Evaluation of NfL in Study Population

Overall, all enrolled COVID-19 patients showed significantly higher plasma NfL levels compared to HD (27.1 [14.4–39.3] and 9.1 [5.7–12.4] pg/mL, $p < 0.0001$) (Figure 2A, Table 1). After stratifying COVID-19 patients into ARDS and non-ARDS groups, higher plasma NfL levels were observed in the ARDS compared to the non-ARDS group (33.8 [18.1–72.2] and 17.8 [10.2–27.6] pg/mL, respectively, $p = 0.0005$) (Figure 2B). Both ARDS and non-ARDS groups showed higher plasma NfL levels compared to HD ($p < 0.0001$ and $p = 0.0212$, respectively) (Figure 2B).

Interestingly, on hospital admission, we observed higher plasma NfL levels in patients that required oxygen support/ventilation during hospitalization (VMK, NIV and IOT) compared to HD (VMK: 26.7 [14.4–32.5], NIV: 29.4 [14.9–59.5], IOT: 39.0 [22.7–93.5]; $p = 0.0258$, $p < 0.0001$ and $p < 0.0001$, respectively) (Supplementary Figure S1A). Conversely, no differences were observed between the AA group and HD (14.8 [6.3–25.4]) (Supplementary Figure S1A). Finally, we observed that NIV and IOT groups showed significantly higher plasma NfL levels compared to the AA group ($p = 0.0088$ and $p = 0.0023$, respectively) (Supplementary Figure S1A).

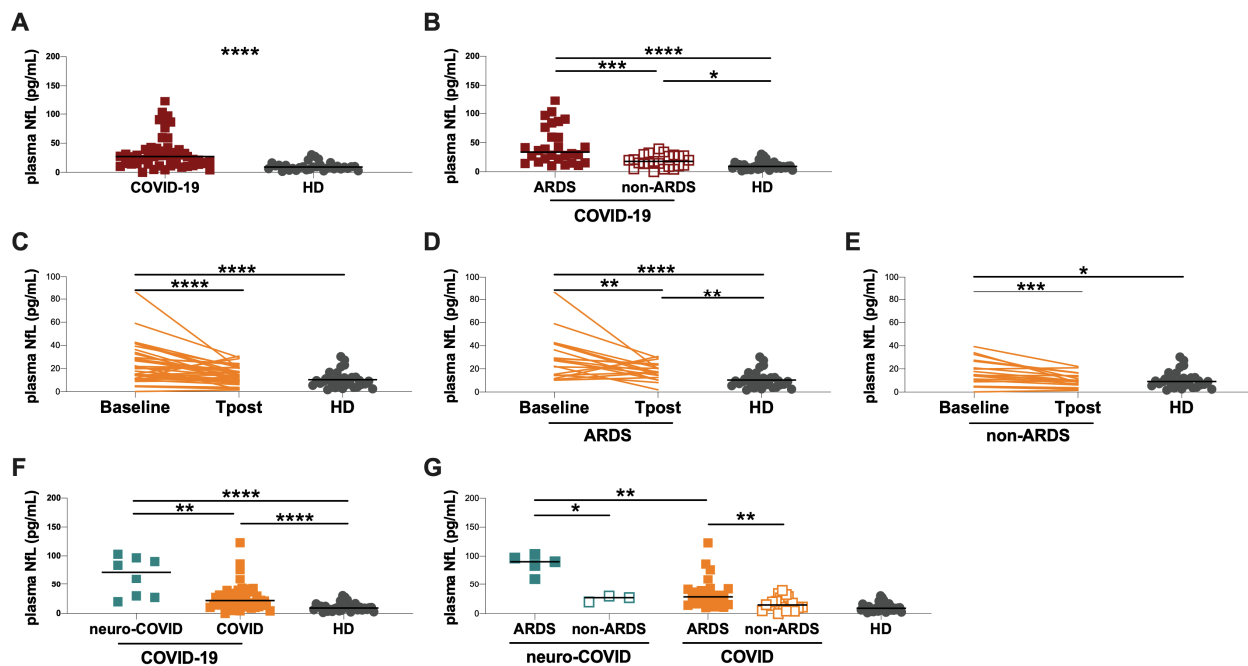


Figure 2. Evaluation of plasma NfL levels in COVID-19 patients and healthy donors. (A) Evaluation of plasma NfL levels in COVID-19 patients and HD. (B) Evaluation of plasma NfL levels in patients with ARDS (ARDS group), patients without ARDS (non-ARDS group) and HD. (C) Longitudinal evaluation of plasma NfL levels in COVID-19 patients. (D) Longitudinal evaluation of plasma NfL levels in COVID-19 patients who developed ARDS during hospitalization. (E) Longitudinal evaluation of plasma NfL levels in COVID-19 patients who did not developed ARDS during hospitalization. (F) Evaluation of plasma NfL levels in COVID-19 patients with severe neurological symptoms (neuro-COVID group), COVID-19 patients without severe neurological symptoms (COVID group) and HD. (G) Evaluation of plasma NfL levels in neuro-COVID and COVID groups stratified according to ARDS. Horizontal lines represent medians. COVID-19: coronavirus disease 2019; neuro-COVID group: COVID-19 patients with severe neurological symptoms; COVID group: COVID-19 patients without severe neurological symptoms; NfL: neurofilament light chain; HD: healthy donors; ARDS: acute respiratory distress syndrome; CSF: cerebrospinal fluid. ****: $p < 0.0001$; ***: $0.0001 < p < 0.001$; **: $0.001 < p < 0.01$; *: $0.01 < p < 0.05$.

COVID-19 patients were further stratified according to the presence comorbidities (Supplementary Table S1). On hospital admission, higher plasma NfL levels in patients with at least one comorbidity compared to those without was observed (29.2 [15.7–59.4] and 20.9 [11.2–29.9] pg/mL, respectively, $p = 0.0436$) (Supplementary Figure S1B). However, both groups (with and without comorbidities) showed higher plasma NfL levels compared to HD ($p < 0.0001$ and $p = 0.0025$, respectively) (Supplementary Figure S1B).

The longitudinal evaluation of plasma NfL levels performed in 38 COVID-19 patients showed a statistically significant decrease at the Tpost compared to baseline (13.8 [8.7–21.1] and 20.4 [11.6–30.2] pg/mL, respectively, $p < 0.0001$) (Figure 2C). At the Tpost, COVID-19 patients showed higher plasma NfL levels compared to HD, although the difference was not statistically significant (Figure 2C). After stratifying patients according to the occurrence of ARDS during hospitalization, at the Tpost, both ARDS and non-ARDS groups showed a reduction of plasma NfL levels compared to baseline (ARDS group: 28.1 [14.9–41.4] and 17.2 [12.6–23.3] pg/mL, respectively, $p = 0.0095$; non-ARDS group: 14.4 [8.9–26.7] and 9.7 [6.1–14.3] pg/mL, respectively, $p = 0.0001$) (Figure 2D and 2E, respectively). However, at the Tpost, plasma NfL levels were still significantly increased in ARDS group compared to HD ($p = 0.0037$) (Figure 2D), whereas no statistically significant differences were observed between non-ARDS group and HD (Figure 2E).

Stratifying COVID-19 patients according to the occurrence of severe neurological symptoms into neuro-COVID and COVID groups, plasma NfL levels were significantly increased in neuro-COVID compared to COVID group (71.7 [27.9–95.1] and 21.8 [13.9–34.0] pg/mL, respectively, $p = 0.0034$) (Figure 2F). Both neuro-COVID and COVID groups showed higher plasma NfL levels compared to HD ($p < 0.0001$ and $p < 0.0001$, respectively) (Figure 2F).

Stratifying neuro-COVID and COVID groups into ARDS and non-ARDS groups, we observed that both neuro-COVID ARDS and COVID ARDS groups showed higher plasma NfL levels than the corresponding non-ARDS groups (neuro-COVID group, ARDS vs. non-ARDS: 90.3 [71.7–99.9] and 27.2 [19.8–29.9] pg/mL, respectively, $p = 0.0357$; COVID group, ARDS vs. non-ARDS: 28.6 [15.3–42.6] and 14.8 [9.2–27.4] pg/mL, respectively, $p = 0.0041$) (Figure 2G). Interestingly, patients from the neuro-COVID ARDS group showed significantly increased plasma NfL levels compared to the COVID ARDS group ($p = 0.0052$) (Figure 2G).

Finally, in the neuro-COVID group, the evaluation of CSF NfL levels showed higher concentrations in the ARDS compared to the non-ARDS group (6480 [1512–11012] and 476 [305–2859] pg/mL, respectively, $p = 0.0260$) (Figure 3A). A positive correlation between NfL levels in CSF and plasma samples was observed ($\rho = 0.8095$, $p = 0.0218$).

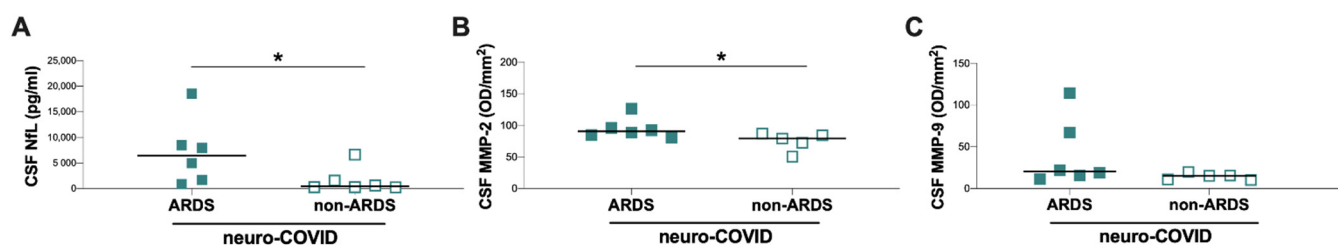


Figure 3. Evaluation of CSF NfL, MMP-2, and MMP-9 levels in neuro-COVID group. (A) Evaluation of CSF NfL levels in COVID-19 patients with severe neurological symptoms (neuro-COVID group) stratified according to ARDS development. (B) Evaluation of CSF MMP-2 levels in COVID-19 patients with neurological symptoms (neuro-COVID group) stratified according to ARDS development. (C) Evaluation of CSF MMP-9 levels in COVID-19 patients with neurological symptoms (neuro-COVID group) stratified according to ARDS development. Horizontal lines represent medians. Neuro-COVID group: COVID-19 patients with severe neurological symptoms; NfL: neurofilament light chain; HD: healthy donors; ARDS: acute respiratory distress syndrome; CSF: cerebrospinal fluid; MMP-2: matrix metalloprotease-2; MMP-9: matrix metalloprotease-9; OD: optical density. *: $0.01 < p < 0.05$.

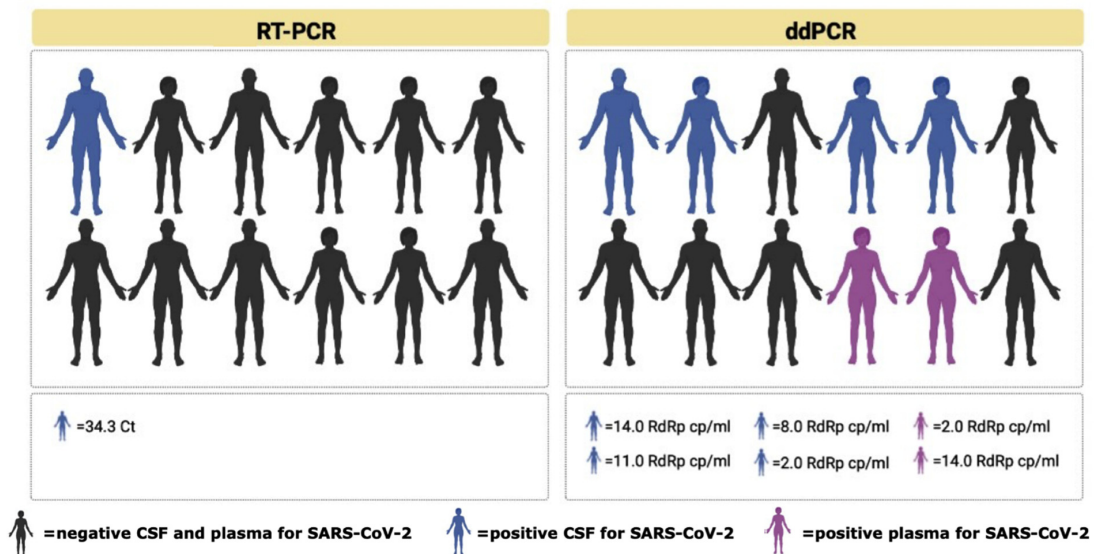
3.3. CSF MMP Levels in Neuro-COVID Group

The zymographic analysis of CSF samples from neuro-COVID-19 patients evidenced on the gel two main lysis bands, present at different levels, with an apparent molecular mass of 72 and 92 kDa, corresponding to MMP-2 and MMP-9, respectively. The quantitative analysis of MMP levels in CSF samples by zymography showed significantly higher CSF MMP-2 levels in the ARDS compared to the non-ARDS group (90.5 [83.5–103.6] and 79.0 [61.4–85.7], respectively, $p = 0.0303$) (Figure 3B) and higher CSF MMP-9 levels, although not statistically significant (MMP-9: 20.5 [14.6–79.0] and 15.2 [10.6–17.8], respectively, $p = 0.0823$) (Figure 3C).

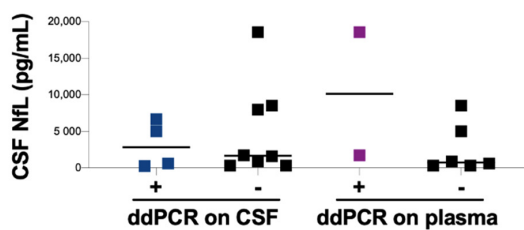
3.4. SARS-CoV-2 RNA Evaluation on CSF and Plasma Samples of Neuro-COVID Patients

For viral RNA detection, real-time RT-PCR and ddPCR were performed in collected CSF samples from neuro-COVID patients. Using RT-PCR, SARS-CoV-2 RNA was detected only in one CSF sample (Figure 4A and Table 3). Conversely, the evaluation of SARS-CoV-2 RNA with ddPCR showed viral RNA detection in the CSF of 4 out of 12 neuro-COVID patients and in plasma of 2 out of 8 neuro-COVID patients (Figure 4A and Table 3).

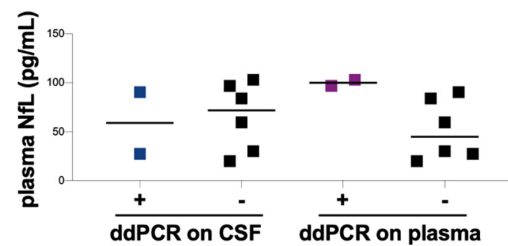
A



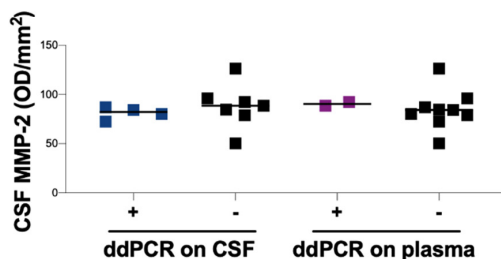
B



C



D



E

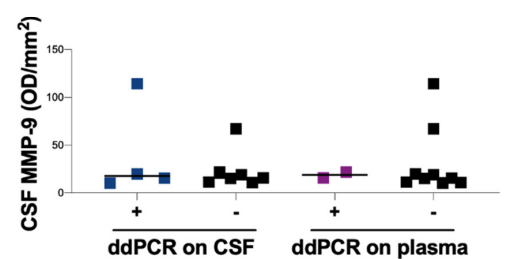


Figure 4. Detection of SARS-CoV-2 RNA on CSF and plasma samples and evaluation of NfL and MMPS levels in neuro-COVID group. (A) Among COVID-19 patients with neurological symptoms (neuro-COVID group), the detection of SARS-CoV-2 RNA on CSF and plasma samples was performed using RT-PCR and ddPCR. (B) Evaluation of CSF NfL levels in COVID-19 patients with severe neurological symptoms (neuro-COVID group) stratified according to ddPCR positivity on CSF and plasma. (C) Evaluation of plasma NfL levels in COVID-19 patients with severe neurological symptoms (neuro-COVID group) stratified according to ddPCR positivity on CSF and plasma. (D) Evaluation of CSF MMP-2 levels in COVID-19 patients with severe neurological symptoms (neuro-COVID group) stratified according to ddPCR positivity on CSF and plasma. (E) Evaluation of CSF MMP-9 levels in COVID-19 patients with severe neurological symptoms (neuro-COVID group) stratified according to ddPCR positivity on CSF and plasma. Horizontal lines represent medians. SARS-CoV-2: severe acute respiratory syndrome coronavirus 2; RT-PCR: reverse transcription-polymerase chain reaction; ddPCR: droplet digital polymerase chain reaction; CSF: cerebrospinal fluid; NfL: neurofilament light chain; MMP-2: matrix metalloprotease-9; MMP-9: matrix metalloprotease-9.

No statistically significant differences in CSF and plasma NfL levels, and CSF MMP-2 and MMP-9 levels, were observed after comparing neuro-COVID patients with and without SARS-CoV-2 RNA detection in CSF and plasma samples (Figure 4B–E).

4. Discussion

Evidence of the effects of SARS-CoV-2 on the CNS is evolving, with the virus being linked to neurological and psychiatric symptoms [17]. Several studies found COVID-19 to be associated with neurological manifestations in up to 36% of patients [49] and the most common reported manifestations were cerebrovascular events, followed by altered mental status [50]. Neurological manifestations can range from a mild headache or “brain fog” [51], to more serious complications such as Guillain-Barre syndrome [52], encephalitis [19], and arterial and venous strokes [53]. Several earliest reports of CNS involvement also described an unusually high rate of anosmia and dysgeusia [50]. The pathogenesis of these CNS effects of COVID-19 is still not known. In line with previous reports [54,55], in our study, we observed higher plasma NfL levels in COVID-19 patients on hospital admission compared to HD, especially in those who developed ARDS during hospitalization. A further stratification according to the maximal oxygen supply/ventilation support required during the hospitalization showed higher plasma NfL levels in patients who required NIV or IOT. Considering that NfL assessment was performed on hospital admission when patients were not yet subjected to ventilation, our data underline the potential role of plasma NfL levels as a prognostic marker of COVID-19 severity. These data are in line with Sutter et al. [55], showing that higher plasma NfL levels are associated with unfavorable short-term outcome in COVID-19 patients. Furthermore, in accordance with Aamodt et al. [56], and Masvekar et al. [57], the evaluation of plasma NfL levels on hospital admission might identify COVID-19 patients with either neurological comorbidities or increased risk of progression to severe COVID-19, thus requiring intensive cares, also focused in preventing further CNS injuries. The identification of a blood biomarker, such as plasma NfL, which is able to assess CNS impairment, could be useful to monitor the severity of the disease and optimize treatment strategies.

In our study, we found that COVID-19 patients with comorbidities showed higher plasma NfL levels on hospital admission compared to those without, although both groups showed higher plasma NfL levels compared to HD. It is not completely clear if comorbidities may impact plasma NfL levels. There is some evidence that plasma NfL levels could be influenced by body mass index (BMI) [58,59], renal function [60], and diabetes [61]. However, as previously showed by Koini et al. [62], the impact that comorbidities could have on plasma NfL levels is influenced by the age of the individual.

Increased plasma NfL levels were found in patients with severe neurological manifestations compared to patients without these symptoms, with the highest increase in neuro-COVID patients who developed ARDS compared to patients who did not. All these data argue in favor of a neuronal damage associated with COVID-19, especially in those patients with severe neurological symptoms and with a severe form of the disease. Furthermore, our data demonstrate increased plasma NfL levels in patients without neurological symptoms at the acute stage of COVID-19, suggesting the presence of subclinical CNS involvement in severe COVID-19 patients. Indeed, Nf is a structural protein that determines axonal caliber and conduction velocity in neurons [63]. One of the three Nf components, the NfL, has been proposed as a biomarker of axonal damage [64]. High CSF NfL levels have been found in patients with neurodegenerative conditions [65–67]. As a less invasive parameter, plasma NfL is supposed to be a surrogate marker, instead of CSF NfL in the evaluation of neural degeneration. Evidence that both CSF and blood NfL may serve as diagnostic, prognostic, and monitoring biomarkers in neurological diseases are progressively accumulating, and NfL is one of the most promising biomarkers to be used in clinical and research settings in the next future [68]. In our study, in line with previously report [35], a positive correlation between CSF and plasma NfL levels was observed, although performed

in a small sample size. These data underline the potential role of plasma NfL evaluation to detect neuro-axonal injury and monitor COVID-19-associated neuronal damage.

The longitudinal evaluation of COVID-19 patients demonstrated that plasma NfL levels significantly decreased three months after discharge. Nevertheless, after recovery from the acute phase of the disease, plasma NfL levels were still altered in patients who developed ARDS during hospitalization, compared to HD. These data are in line with a recent report by Hampshire et al. [69], showing that severe COVID-19 illness is associated with objectively relevant measurable cognitive deficits that persist into the chronic phase. Thus, as already proven for multiple sclerosis, Alzheimer, and Parkinson disease [70,71], the persistence of high plasma NfL levels in patients with COVID-19 during the post-acute phase of the disease could represent a biomarker of neurocognitive impairment. In perspective, it will be useful to correlate plasma NfL levels with long-COVID clinical manifestations.

In our study, the high levels of CSF NfL, MMP-2, and MMP-9 observed in neuro-COVID with ARDS could be the expression of neuronal damage and BBB disruption possibly induced by the altered blood flow in the CNS and hypoxia. MMPs have been widely investigated for their role in the disruption of the BBB, particularly through the degradation of the components of the basal lamina, following stroke [72–74] and other cerebral pathologies such as traumatic brain injury [75]. However, a recent report has suggested that CSF MMP-9 levels were quantitatively linked to the amount of NfL release [76]. Indeed, MMPs are effector molecules of tissue damage that are released as a consequence of pro-inflammatory cytokine secretion [77,78]. MMPs can activate and regulate cytokine signaling in a positive feedback loop, enhancing the excessive inflammation [79–81]. This evidence underlines the role of MMPs not only in disrupting BBB integrity facilitating extravasation into the CNS, but also in promoting glial and neuronal cell death with the consequent increase in NfL levels. From a clinical point of view, the consequences of these mechanisms could be the development of neurological sequelae [82,83].

Our results are consistent with previous data showing that MMP-2 (more than MMP-9) plays a critical role in BBB disruption, glial cell activation, and white matter damages after chronic cerebral hypoperfusion in animal models and patients with cardiac arrest [84,85]. Indeed, in COVID-19 patients, CNS hypoxia can be a consequence of respiratory failure, thrombotic microangiopathy, and indirect effects of the vigorous inflammatory response with extensive cytokine activation. As suggested by Mohammadhosayni et al. [86], the high levels of inflammatory cytokines, such as TNF- α , might help to increase the production of MMPs, leading to BBB disruption in COVID-19 patients with neurological symptoms.

To date, is still unclear whether the amount of NfL crossing the BBB is dependent on the integrity of this barrier [87]. NfL is produced as a direct result of neuroaxonal injury but not as a direct result of BBB compromise per se. Impairment of BBB integrity can potentially facilitate NfL release out of the CNS into blood. However, as reported by other authors [88,89], in multiple sclerosis patients, where chronic inflammation leads to the disruption of the BBB, NfL does not systematically correlate with BBB integrity. Mechanistic studies are needed to establish causative precedence but is plausible that the loss of integrity of the BBB increases permeability of pre-existing NfL from CNS into blood.

Finally, in this manuscript, we have also addressed the issue of SARS-CoV-2 RNA detection in CSF and plasma samples of patients with severe neurological symptoms. These results were obtained using ddPCR, a highly sensitive method for nucleic acids quantification, compared to real-time RT-PCR. In the clinical practice, the gold standard for the detection and quantification of SARS-CoV-2 RNA is the real-time RT-PCR. Recently, attention has been focused on the use of ddPCR system for the detection and quantification of SARS-CoV-2 RNA. This assay provides a reliable absolute quantification of viral RNA and is endowed with a higher sensitivity compared to real-time RT-PCR, specifically for quantifying low viral loads [90,91]. Indeed, in our study, only one out of twelve CSF sample showed SARS-CoV-2 RNA detection using real-time RT-PCR, whereas four out of twelve CSF samples showed SARS-CoV-2 RNA positivity using ddPCR. Moreover, the RT-PCR positive CSF sample showed the highest viral load when assessed with the ddPCR. Of note,

for the four patients with SARS-CoV-2 RNA ddPCR detection in the CSF, the corresponding plasma samples tested negative (using the same molecular method), therefore, a viral carry-over from the blood to the CNS seems unlikely. From the comparison of the two methods, as expected, we observed a better performance of ddPCR respect to real-time RT-PCR, suggesting that ddPCR can represent an added value in reducing false negative results and in detecting very low concentrations of viral RNA. These characteristics can represent a useful tool for better identifying viral dissemination in extra-pulmonary regions and in turn can unravel its significance in terms of virus transmissibility and extra-pulmonary clinical manifestations. Even if the *in vitro* replication of SARS-CoV-2 in neural cells has been widely reported [92–94], a limit of ddPCR (and also of RT-PCR) is that the detection of SARS-CoV-2 RNA is not equal to identification of effectively infectious viral particles, so these methods are not informative about active viral replication but only on the presence of viral RNA.

In our cohort, no statistically significant differences were observed in CSF NfL levels as well as in CSF MMP-2 and MMP-9 levels after stratifying patients with severe neurological symptoms according to SARS-CoV-2 RNA detection by ddPCR on either CSF or plasma samples. This aspect, together with the increased NfL levels observed in ARDS patients, suggests that CNS damage is prevalently associated with COVID-19 severity rather than SARS-CoV-2 RNA detection. This is in line with the evidence obtained by other authors, showing that neurological signs and symptoms could be the effect of hyperinflammation and hypoxia [91]. Nevertheless, our data evidenced the ability of SARS-CoV-2 to invade the CNS. SARS-CoV-2 infection of human host cells is mediated mainly by the cellular receptor ACE-2, which is expressed at very low levels in the CNS under normal conditions [95]. To date, several reports on potential neuroinvasion by SARS-CoV-2 appeared in the literature although most of them were conducted on animal models [94,96,97]. We should also consider that the presence of viral RNA does not directly correspond to the presence of viable viral particles, which should be assessed with viral isolation in cultured cells.

In summary, our data suggest CNS damage in COVID-19 patients during the acute phase of the disease, which is mainly related to COVID-19 severity rather than SARS-CoV-2 neuro-invasion. COVID-19 patients who developed ARDS during the acute phase of the disease tended to maintain higher levels of NfL compared to HD, up to three months after hospital discharge. Measurement of NfL levels in plasma samples represents a convenient and easy to perform method to assess neuronal damage in the context of COVID-19. As NfL is specific for neuronal damage, the increased plasma NfL levels in patients without neurological symptoms suggest the presence of subclinical CNS involvement in COVID-19 patients, especially in those with the most severe forms of the disease. The implications of this subclinical CNS involvement need to be further elucidated and correlated with long-COVID manifestations.

5. Conclusions

A growing number of COVID-19 patients showed neurologic symptoms during the acute stage of the disease as well as several neurological sequelae following COVID-19 recovery. To our knowledge, this is the first study providing a CNS damage and alteration of BBB integrity in COVID-19 patients with severe neurological symptoms during the acute phase of the disease, which is mainly related to COVID-19 severity rather than SARS-CoV-2 neuro-invasion. COVID-19 patients who developed ARDS during the acute phase of the disease tended to maintain high levels of NfL, up to three months after hospital discharge. Measurement of NfL levels in plasma samples represents a convenient and easy to perform method to assess neuronal damage in the context of COVID-19.

Supplementary Materials: The following supporting information can be downloaded at: <https://www.mdpi.com/xxx/s1>, Figure S1: Evaluation of plasma NfL levels on hospital admission in COVID-19 patients stratified according to the presence of comorbidities and maximal ventilation needed during hospitalization; Table S1: Plasma NfL levels on hospital admission, comorbidities and maximal ventilation needed during hospitalization in COVID-19 patients.

Author Contributions: Conceptualization: M.A.Z. and M.R.C.; Formal analysis: M.A.Z., L.P., T.L., L.M. and L.D.; Investigation: All authors; Resources: All authors; Writing—original draft: M.A.Z., M.I. and T.L.; Writing—review and editing: All authors; Visualization: M.A.Z. All authors have read and agreed to the published version of the manuscript.

Funding: This study was supported by Sapienza University of Rome: Ricerca Ateneo Sapienza–Avvio alla Ricerca (protocol number AR22117A87088A29).

Institutional Review Board Statement: The study was conducted in accordance with the Declaration of Helsinki, and approved by the Ethics Committee of Policlinico Umberto I, Sapienza University of Rome (protocol number 298/2020), and the Ethics Committee of Fondazione Policlinico Tor Vergata (protocol number 46.20).

Informed Consent Statement: Each subject gave written informed consent for participation to the study.

Data Availability Statement: All data generated or analyzed during this study are included in this published article. The datasets used and/or analyzed during the current study are available from the corresponding author on reasonable request.

Acknowledgments: The authors would like to acknowledge Federica Dominelli (Sapienza University of Rome), Mariasilvia Guardiani (Sapienza University of Rome), Eeva Tortellini (Sapienza University of Rome), Stefano D’Anna (Tor Vergata University of Rome), and Rossana Scutari (Tor Vergata University of Rome) for their technical support.

Conflicts of Interest: The authors declare no conflict of interest.

References

- Gupta, A.; Madhavan, M.V.; Sehgal, K.; Nair, N.; Mahajan, S.; Sehrawat, T.S.; Bikdeli, B.; Ahluwalia, N.; Ausiello, J.C.; Wan, E.Y.; et al. Extrapulmonary Manifestations of COVID-19. *Nat. Med.* **2020**, *26*, 1017–1032. [[CrossRef](#)] [[PubMed](#)]
- Guan, W.-J.; Ni, Z.-Y.; Hu, Y.; Liang, W.-H.; Ou, C.-Q.; He, J.-X.; Liu, L.; Shan, H.; Lei, C.-L.; Hui, D.S.C.; et al. Clinical Characteristics of Coronavirus Disease 2019 in China. *N. Engl. J. Med.* **2020**, *382*, 1708–1720. [[CrossRef](#)] [[PubMed](#)]
- Shi, S.; Qin, M.; Shen, B.; Cai, Y.; Liu, T.; Yang, F.; Gong, W.; Liu, X.; Liang, J.; Zhao, Q.; et al. Association of Cardiac Injury With Mortality in Hospitalized Patients with COVID-19 in Wuhan, China. *JAMA Cardiol.* **2020**, *5*, 802–810. [[CrossRef](#)] [[PubMed](#)]
- Zhou, F.; Yu, T.; Du, R.; Fan, G.; Liu, Y.; Liu, Z.; Xiang, J.; Wang, Y.; Song, B.; Gu, X.; et al. Clinical Course and Risk Factors for Mortality of Adult Inpatients with COVID-19 in Wuhan, China: A Retrospective Cohort Study. *Lancet* **2020**, *395*, 1054–1062. [[CrossRef](#)]
- Wu, C.; Chen, X.; Cai, Y.; Xia, J.; Zhou, X.; Xu, S.; Huang, H.; Zhang, L.; Zhou, X.; Du, C.; et al. Risk Factors Associated With Acute Respiratory Distress Syndrome and Death in Patients with Coronavirus Disease 2019 Pneumonia in Wuhan, China. *JAMA Intern. Med.* **2020**, *180*, 934–943. [[CrossRef](#)]
- Pasculli, P.; Zingaropoli, M.A.; Masci, G.M.; Mazzuti, L.; Perri, V.; Paribeni, F.; Russo, G.; Arcari, G.; Iafrate, F.; Vullo, F.; et al. Chest Computed Tomography Score, Cycle Threshold Values and Secondary Infection in Predicting COVID-19 Mortality. *New Microbiol.* **2021**, *44*, 145–154.
- Huang, C.; Wang, Y.; Li, X.; Ren, L.; Zhao, J.; Hu, Y.; Zhang, L.; Fan, G.; Xu, J.; Gu, X.; et al. Clinical Features of Patients Infected with 2019 Novel Coronavirus in Wuhan, China. *Lancet* **2020**, *395*, 497–506. [[CrossRef](#)]
- Wang, D.; Hu, B.; Hu, C.; Zhu, F.; Liu, X.; Zhang, J.; Wang, B.; Xiang, H.; Cheng, Z.; Xiong, Y.; et al. Clinical Characteristics of 138 Hospitalized Patients With 2019 Novel Coronavirus-Infected Pneumonia in Wuhan, China. *JAMA* **2020**, *323*, 1061–1069. [[CrossRef](#)]
- Lechien, J.R.; Chiesa-Estomba, C.M.; De Siati, D.R.; Horoi, M.; Le Bon, S.D.; Rodriguez, A.; Dequanter, D.; Blecic, S.; El Afia, F.; Distinguin, L.; et al. Olfactory and Gustatory Dysfunctions as a Clinical Presentation of Mild-to-Moderate Forms of the Coronavirus Disease (COVID-19): A Multicenter European Study. *Eur. Arch. Otorhinolaryngol.* **2020**, *277*, 2251–2261. [[CrossRef](#)]
- Spinato, G.; Fabbris, C.; Polesel, J.; Cazzador, D.; Borsetto, D.; Hopkins, C.; Boscolo-Rizzo, P. Alterations in Smell or Taste in Mildly Symptomatic Outpatients with SARS-CoV-2 Infection. *JAMA* **2020**, *323*, 2089–2090. [[CrossRef](#)]
- Oxley, T.J.; Mocco, J.; Majidi, S.; Kellner, C.P.; Shoirah, H.; Singh, I.P.; De Leacy, R.A.; Shigematsu, T.; Ladner, T.R.; Yaeger, K.A.; et al. Large-Vessel Stroke as a Presenting Feature of Covid-19 in the Young. *N. Engl. J. Med.* **2020**, *382*, e60. [[CrossRef](#)] [[PubMed](#)]
- Yaghi, S.; Ishida, K.; Torres, J.; Mac Grory, B.; Raz, E.; Humbert, K.; Henninger, N.; Trivedi, T.; Lillemo, K.; Alam, S.; et al. SARS-CoV-2 and Stroke in a New York Healthcare System. *Stroke* **2020**, *51*, 2002–2011. [[CrossRef](#)] [[PubMed](#)]
- Lan, J.; Ge, J.; Yu, J.; Shan, S.; Zhou, H.; Fan, S.; Zhang, Q.; Shi, X.; Wang, Q.; Zhang, L.; et al. Structure of the SARS-CoV-2 Spike Receptor-Binding Domain Bound to the ACE2 Receptor. *Nature* **2020**, *581*, 215–220. [[CrossRef](#)]
- Lei, C.; Qian, K.; Li, T.; Zhang, S.; Fu, W.; Ding, M.; Hu, S. Neutralization of SARS-CoV-2 Spike Pseudotyped Virus by Recombinant ACE2-Ig. *Nat. Commun.* **2020**, *11*, 2070. [[CrossRef](#)]

15. Zhao, H.; Shen, D.; Zhou, H.; Liu, J.; Chen, S. Guillain-Barré Syndrome Associated with SARS-CoV-2 Infection: Causality or Coincidence? *Lancet Neurol.* **2020**, *19*, 383–384. [[CrossRef](#)]
16. Toscano, G.; Palmerini, F.; Ravaglia, S.; Ruiz, L.; Invernizzi, P.; Cuzzoni, M.G.; Franciotta, D.; Baldanti, F.; Daturi, R.; Postorino, P.; et al. Guillain-Barré Syndrome Associated with SARS-CoV-2. *N. Engl. J. Med.* **2020**, *382*, 2574–2576. [[CrossRef](#)]
17. Helms, J.; Kremer, S.; Merdji, H.; Clere-Jehl, R.; Schenck, M.; Kummerlen, C.; Collange, O.; Boulay, C.; Fafi-Kremer, S.; Ohana, M.; et al. Neurologic Features in Severe SARS-CoV-2 Infection. *N. Engl. J. Med.* **2020**, *382*, 2268–2270. [[CrossRef](#)]
18. Franceschi, A.M.; Ahmed, O.; Giliberto, L.; Castillo, M. Hemorrhagic Posterior Reversible Encephalopathy Syndrome as a Manifestation of COVID-19 Infection. *AJNR Am. J. Neuroradiol.* **2020**, *41*, 1173–1176. [[CrossRef](#)]
19. Moriguchi, T.; Harii, N.; Goto, J.; Harada, D.; Sugawara, H.; Takamino, J.; Ueno, M.; Sakata, H.; Kondo, K.; Myose, N.; et al. A First Case of Meningitis/Encephalitis Associated with SARS-Coronavirus-2. *Int. J. Infect. Dis.* **2020**, *94*, 55–58. [[CrossRef](#)]
20. Poyiadji, N.; Shahin, G.; Noujaim, D.; Stone, M.; Patel, S.; Griffith, B. COVID-19-Associated Acute Hemorrhagic Necrotizing Encephalopathy: Imaging Features. *Radiology* **2020**, *296*, E119–E120. [[CrossRef](#)]
21. Marinho, P.M.; Marcos, A.A.A.; Romano, A.C.; Nascimento, H.; Belfort, R. Retinal Findings in Patients with COVID-19. *Lancet* **2020**, *395*, 1610. [[CrossRef](#)]
22. Wu, P.; Duan, F.; Luo, C.; Liu, Q.; Qu, X.; Liang, L.; Wu, K. Characteristics of Ocular Findings of Patients With Coronavirus Disease 2019 (COVID-19) in Hubei Province, China. *JAMA Ophthalmol.* **2020**, *138*, 575–578. [[CrossRef](#)] [[PubMed](#)]
23. Cheema, M.; Aghazadeh, H.; Nazarali, S.; Ting, A.; Hodges, J.; McFarlane, A.; Kanji, J.N.; Zelyas, N.; Damji, K.F.; Solarte, C. Keratoconjunctivitis as the Initial Medical Presentation of the Novel Coronavirus Disease 2019 (COVID-19). *Can. J. Ophthalmol.* **2020**, *55*, e125–e129. [[CrossRef](#)] [[PubMed](#)]
24. Liu, J.-M.; Tan, B.-H.; Wu, S.; Gui, Y.; Suo, J.-L.; Li, Y.-C. Evidence of Central Nervous System Infection and Neuroinvasive Routes, as Well as Neurological Involvement, in the Lethality of SARS-CoV-2 Infection. *J. Med. Virol.* **2021**, *93*, 1304–1313. [[CrossRef](#)]
25. Domingues, R.B.; Lakeman, F.D.; Mayo, M.S.; Whitley, R.J. Application of Competitive PCR to Cerebrospinal Fluid Samples from Patients with Herpes Simplex Encephalitis. *J. Clin. Microbiol.* **1998**, *36*, 2229–2234. [[CrossRef](#)]
26. Huang, Y.H.; Jiang, D.; Huang, J.T. SARS-CoV-2 Detected in Cerebrospinal Fluid by PCR in a Case of COVID-19 Encephalitis. *Brain Behav. Immun.* **2020**, *87*, 149. [[CrossRef](#)]
27. Kremer, S.; Lersy, F.; de Sèze, J.; Ferré, J.-C.; Maamar, A.; Carsin-Nicol, B.; Collange, O.; Bonneville, F.; Adam, G.; Martin-Blondel, G.; et al. Brain MRI Findings in Severe COVID-19: A Retrospective Observational Study. *Radiology* **2020**, *297*, E242–E251. [[CrossRef](#)]
28. Filatov, A.; Sharma, P.; Hindi, F.; Espinosa, P.S. Neurological Complications of Coronavirus Disease (COVID-19): Encephalopathy. *Cureus* **2020**, *12*, e7352. [[CrossRef](#)]
29. Schaller, T.; Hirschtbühl, K.; Burkhardt, K.; Braun, G.; Trepel, M.; Märkl, B.; Claus, R. Postmortem Examination of Patients with COVID-19. *JAMA* **2020**, *323*, 2518–2520. [[CrossRef](#)]
30. Teunissen, C.E.; Khalil, M. Neurofilaments as Biomarkers in Multiple Sclerosis. *Mult. Scler.* **2012**, *18*, 552–556. [[CrossRef](#)]
31. Hendricks, R.; Baker, D.; Brumm, J.; Davancaze, T.; Harp, C.; Herman, A.; Büdingen, H.-C.von; Townsend, M.; Fischer, S.K. Establishment of Neurofilament Light Chain Simoa Assay in Cerebrospinal Fluid and Blood. *Bioanalysis* **2019**, *11*, 1405–1418. [[CrossRef](#)] [[PubMed](#)]
32. Steinacker, P.; Feneberg, E.; Weishaupt, J.; Bretschneider, J.; Tumani, H.; Andersen, P.M.; von Arnim, C.A.F.; Böhm, S.; Kassubek, J.; Kubisch, C.; et al. Neurofilaments in the Diagnosis of Motoneuron Diseases: A Prospective Study on 455 Patients. *J. Neurol. Neurosurg. Psychiatry* **2016**, *87*, 12–20. [[CrossRef](#)] [[PubMed](#)]
33. Kovacs, G.G.; Andreasson, U.; Liman, V.; Regelsberger, G.; Lutz, M.I.; Danics, K.; Keller, E.; Zetterberg, H.; Blennow, K. Plasma and Cerebrospinal Fluid Tau and Neurofilament Concentrations in Rapidly Progressive Neurological Syndromes: A Neuropathology-Based Cohort. *Eur. J. Neurol.* **2017**, *24*, 1326–e77. [[CrossRef](#)]
34. Thompson, A.G.B.; Luk, C.; Heslegrave, A.J.; Zetterberg, H.; Mead, S.H.; Collinge, J.; Jackson, G.S. Neurofilament Light Chain and Tau Concentrations Are Markedly Increased in the Serum of Patients with Sporadic Creutzfeldt-Jakob Disease, and Tau Correlates with Rate of Disease Progression. *J. Neurol. Neurosurg. Psychiatry* **2018**, *89*, 955–961. [[CrossRef](#)]
35. Khalil, M.; Teunissen, C.E.; Otto, M.; Piehl, F.; Sormani, M.P.; Gattringer, T.; Barro, C.; Kappos, L.; Comabella, M.; Fazekas, F.; et al. Neurofilaments as Biomarkers in Neurological Disorders. *Nat. Rev. Neurol.* **2018**, *14*, 577–589. [[CrossRef](#)] [[PubMed](#)]
36. Cabral-Pacheco, G.A.; Garza-Veloz, I.; Castruita-De la Rosa, C.; Ramirez-Acuña, J.M.; Perez-Romero, B.A.; Guerrero-Rodriguez, J.F.; Martinez-Avila, N.; Martinez-Fierro, M.L. The Roles of Matrix Metalloproteinases and Their Inhibitors in Human Diseases. *Int. J. Mol. Sci.* **2020**, *21*, 9739. [[CrossRef](#)]
37. Spindler, K.R.; Hsu, T.-H. Viral Disruption of the Blood-Brain Barrier. *Trends Microbiol.* **2012**, *20*, 282–290. [[CrossRef](#)]
38. Kolb, S.A.; Lahrtz, F.; Paul, R.; Leppert, D.; Nadal, D.; Pfister, H.W.; Fontana, A. Matrix Metalloproteinases and Tissue Inhibitors of Metalloproteinases in Viral Meningitis: Upregulation of MMP-9 and TIMP-1 in Cerebrospinal Fluid. *J. Neuroimmunol.* **1998**, *84*, 143–150. [[CrossRef](#)]
39. Lind, L.; Eriksson, K.; Grahn, A. Chemokines and Matrix Metalloproteinases in Cerebrospinal Fluid of Patients with Central Nervous System Complications Caused by Varicella-Zoster Virus. *J. Neuroinflamm.* **2019**, *16*, 42. [[CrossRef](#)]
40. Liuzzi, G.M.; Mastroianni, C.M.; Santacroce, M.P.; Fanelli, M.; D’Agostino, C.; Vullo, V.; Riccio, P. Increased Activity of Matrix Metalloproteinases in the Cerebrospinal Fluid of Patients with HIV-Associated Neurological Diseases. *J. Neurovirol.* **2000**, *6*, 156–163. [[CrossRef](#)]

41. Zhou, J.; Stohlman, S.A.; Atkinson, R.; Hinton, D.R.; Marten, N.W. Matrix Metalloproteinase Expression Correlates with Virulence Following Neurotropic Mouse Hepatitis Virus Infection. *J. Virol.* **2002**, *76*, 7374–7384. [[CrossRef](#)] [[PubMed](#)]
42. Di Carlo, D.; Mazzuti, L.; Sciandra, I.; Guerrizio, G.; Oliveto, G.; Riveros Cabral, R.J.; Zingaropoli, M.A.; Turriziani, O. Comparison of FTD SARS-CoV-2 Assay and RealStar RT-PCR Kit 1.0 for the Detection of SARS-CoV-2. *J. Virol. Methods* **2021**, *298*, 114276. [[CrossRef](#)] [[PubMed](#)]
43. Ranieri, V.M.; Rubenfeld, G.D.; Thompson, B.T.; Ferguson, N.D.; Caldwell, E.; Fan, E.; Camporota, L.; Slutsky, A.S.; ARDS Definition Task Force. Acute Respiratory Distress Syndrome: The Berlin Definition. *JAMA* **2012**, *307*, 2526–2533. [[CrossRef](#)] [[PubMed](#)]
44. Ferrazzano, G.; Zingaropoli, M.A.; Costanzo, M.; Belvisi, D.; Dominelli, F.; Pasculli, P.; Ciardi, M.R.; Fabbrini, G.; Defazio, G.; Berardelli, A.; et al. Neurofilament Assessment in Patients with Cervical Dystonia. *Parkinsonism Relat. Disord.* **2022**, *98*, 70–71. [[CrossRef](#)] [[PubMed](#)]
45. Iannetta, M.; Zingaropoli, M.A.; Latronico, T.; Pati, I.; Pontecorvo, S.; Prezioso, C.; Pietropaolo, V.; Cortese, A.; Frontoni, M.; D'Agostino, C.; et al. Dynamic Changes of MMP-9 Plasma Levels Correlate with JCV Reactivation and Immune Activation in Natalizumab-Treated Multiple Sclerosis Patients. *Sci. Rep.* **2019**, *9*, 311. [[CrossRef](#)]
46. Oliva, A.; Cancelli, F.; Brogi, A.; Curtolo, A.; Savelloni, G.; Siccardi, G.; Marcelli, G.; Mazzuti, L.; Ricci, P.; Turriziani, O.; et al. Convalescent Plasma for Haematological Patients with SARS-CoV-2 Pneumonia and Severe Depletion of B-Cell Lymphocytes Following Anti-CD20 Therapy: A Single-Centre Experience and Review of the Literature. *New Microbiol.* **2022**, *45*, 62–72.
47. Alteri, C.; Cento, V.; Antonello, M.; Colagrossi, L.; Merli, M.; Ughi, N.; Renica, S.; Matarazzo, E.; Di Ruscio, F.; Tartaglione, L.; et al. Detection and Quantification of SARS-CoV-2 by Droplet Digital PCR in Real-Time PCR Negative Nasopharyngeal Swabs from Suspected COVID-19 Patients. *PLoS ONE* **2020**, *15*, e0236311. [[CrossRef](#)]
48. Scutari, R.; Piermatteo, L.; Ciancio Manuelli, M.; Iannetta, M.; Salpini, R.; Bertoli, A.; Alteri, C.; Saccomandi, P.; Bellocchi, M.C.; Malagnino, V.; et al. Long-Term SARS-CoV-2 Infection Associated with Viral Dissemination in Different Body Fluids Including Bile in Two Patients with Acute Cholecystitis. *Life* **2020**, *10*, 302. [[CrossRef](#)]
49. Mao, L.; Jin, H.; Wang, M.; Hu, Y.; Chen, S.; He, Q.; Chang, J.; Hong, C.; Zhou, Y.; Wang, D.; et al. Neurologic Manifestations of Hospitalized Patients With Coronavirus Disease 2019 in Wuhan, China. *JAMA Neurol.* **2020**, *77*, 683–690. [[CrossRef](#)]
50. Varatharaj, A.; Thomas, N.; Ellul, M.A.; Davies, N.W.S.; Pollak, T.A.; Tenorio, E.L.; Sultan, M.; Easton, A.; Breen, G.; Zandi, M.; et al. Neurological and Neuropsychiatric Complications of COVID-19 in 153 Patients: A UK-Wide Surveillance Study. *Lancet Psychiatry* **2020**, *7*, 875–882. [[CrossRef](#)]
51. Nauen, D.W.; Hooper, J.E.; Stewart, C.M.; Solomon, I.H. Assessing Brain Capillaries in Coronavirus Disease 2019. *JAMA Neurol.* **2021**, *78*, 760–762. [[CrossRef](#)] [[PubMed](#)]
52. Alberti, P.; Beretta, S.; Piatti, M.; Karantzoulis, A.; Piatti, M.L.; Santoro, P.; Viganò, M.; Giovannelli, G.; Pirro, F.; Montisano, D.A.; et al. Guillain-Barré Syndrome Related to COVID-19 Infection. *Neurol. Neuroimmunol. Neuroinflamm.* **2020**, *7*, e741. [[CrossRef](#)] [[PubMed](#)]
53. Kananeh, M.F.; Thomas, T.; Sharma, K.; Herpich, F.; Urtecho, J.; Athar, M.K.; Jabbour, P.; Shah, S.O. Arterial and Venous Strokes in the Setting of COVID-19. *J. Clin. Neurosci.* **2020**, *79*, 60–66. [[CrossRef](#)] [[PubMed](#)]
54. De Lorenzo, R.; Loré, N.I.; Finardi, A.; Mandelli, A.; Cirillo, D.M.; Tresoldi, C.; Benedetti, F.; Ciceri, F.; Rovere-Querini, P.; Comi, G.; et al. Blood Neurofilament Light Chain and Total Tau Levels at Admission Predict Death in COVID-19 Patients. *J. Neurol.* **2021**, *268*, 4436–4442. [[CrossRef](#)] [[PubMed](#)]
55. Sutter, R.; Hert, L.; De Marchis, G.M.; Twerenbold, R.; Kappos, L.; Naegelin, Y.; Kuster, G.M.; Benkert, P.; Jost, J.; Maceski, A.M.; et al. Serum Neurofilament Light Chain Levels in the Intensive Care Unit: Comparison between Severely Ill Patients with and without Coronavirus Disease 2019. *Ann. Neurol.* **2021**, *89*, 610–616. [[CrossRef](#)]
56. Aamodt, A.H.; Høgestøl, E.A.; Popperud, T.H.; Holter, J.C.; Dyrhol-Riise, A.M.; Tonby, K.; Stiksrud, B.; Quist-Paulsen, E.; Berge, T.; Barratt-Due, A.; et al. Blood Neurofilament Light Concentration at Admittance: A Potential Prognostic Marker in COVID-19. *J. Neurol.* **2021**, *268*, 3574–3583. [[CrossRef](#)]
57. Masvekar, R.R.; Kosa, P.; Jin, K.; Dobbs, K.; Stack, M.A.; Castagnoli, R.; Quaresima, V.; Su, H.C.; Imberti, L.; Notarangelo, L.D.; et al. Prognostic Value of Serum/Plasma Neurofilament Light Chain for COVID-19 Associated Mortality. *medRxiv* **2022**, *9*, 622–632. [[CrossRef](#)]
58. Manouchehrinia, A.; Piehl, F.; Hillert, J.; Kuhle, J.; Alfredsson, L.; Olsson, T.; Kockum, I. Confounding Effect of Blood Volume and Body Mass Index on Blood Neurofilament Light Chain Levels. *Ann. Clin. Transl. Neurol.* **2020**, *7*, 139–143. [[CrossRef](#)]
59. Nilsson, I.A.K.; Millischer, V.; Karrenbauer, V.D.; Juréus, A.; Salehi, A.M.; Norring, C.; von Hausswolff-Juhlin, Y.; Schalling, M.; Blennow, K.; Bulik, C.M.; et al. Plasma Neurofilament Light Chain Concentration Is Increased in Anorexia Nervosa. *Transl. Psychiatry* **2019**, *9*, 180. [[CrossRef](#)]
60. Akamine, S.; Marutani, N.; Kanayama, D.; Gotoh, S.; Maruyama, R.; Yanagida, K.; Sakagami, Y.; Mori, K.; Adachi, H.; Kozawa, J.; et al. Renal Function Is Associated with Blood Neurofilament Light Chain Level in Older Adults. *Sci. Rep.* **2020**, *10*, 20350. [[CrossRef](#)]
61. Thota, R.N.; Chatterjee, P.; Pedrini, S.; Hone, E.; Ferguson, J.J.A.; Garg, M.L.; Martins, R.N. Association of Plasma Neurofilament Light Chain With Glycaemic Control and Insulin Resistance in Middle-Aged Adults. *Front. Endocrinol.* **2022**, *13*, 915449. [[CrossRef](#)] [[PubMed](#)]

62. Koini, M.; Pirpamer, L.; Hofer, E.; Buchmann, A.; Pinter, D.; Ropele, S.; Enzinger, C.; Benkert, P.; Leppert, D.; Kuhle, J.; et al. Factors Influencing Serum Neurofilament Light Chain Levels in Normal Aging. *Aging* **2021**, *13*, 25729–25738. [[CrossRef](#)] [[PubMed](#)]
63. Hoffman, P.N.; Cleveland, D.W.; Griffin, J.W.; Landes, P.W.; Cowan, N.J.; Price, D.L. Neurofilament Gene Expression: A Major Determinant of Axonal Caliber. *Proc. Natl. Acad. Sci. USA* **1987**, *84*, 3472–3476. [[CrossRef](#)] [[PubMed](#)]
64. Norgren, N.; Rosengren, L.; Stigbrand, T. Elevated Neurofilament Levels in Neurological Diseases. *Brain Res.* **2003**, *987*, 25–31. [[CrossRef](#)]
65. Olsson, T.; Barcellos, L.F.; Alfredsson, L. Interactions between Genetic, Lifestyle and Environmental Risk Factors for Multiple Sclerosis. *Nat. Rev. Neurol.* **2017**, *13*, 25–36. [[CrossRef](#)]
66. Skillbäck, T.; Farahmand, B.; Bartlett, J.W.; Rosén, C.; Mattsson, N.; Nägga, K.; Kilander, L.; Religa, D.; Wimo, A.; Winblad, B.; et al. CSF Neurofilament Light Differs in Neurodegenerative Diseases and Predicts Severity and Survival. *Neurology* **2014**, *83*, 1945–1953. [[CrossRef](#)]
67. Karantali, E.; Kazis, D.; Chatzikonstantinou, S.; Petridis, F.; Mavroudis, I. The Role of Neurofilament Light Chain in Frontotemporal Dementia: A Meta-Analysis. *Aging Clin. Exp. Res.* **2021**, *33*, 869–881. [[CrossRef](#)]
68. Kalil, A.C.; Patterson, T.F.; Mehta, A.K.; Tomashek, K.M.; Wolfe, C.R.; Ghazaryan, V.; Marconi, V.C.; Ruiz-Palacios, G.M.; Hsieh, L.; Kline, S.; et al. Baricitinib plus Remdesivir for Hospitalized Adults with Covid-19. *N. Engl. J. Med.* **2021**, *384*, 795–807. [[CrossRef](#)]
69. Hampshire, A.; Chatfield, D.A.; MPhil, A.M.; Jolly, A.; Trender, W.; Hellyer, P.J.; Giovane, M.D.; Newcombe, V.F.J.; Outtrim, J.G.; Warne, B.; et al. Multivariate Profile and Acute-Phase Correlates of Cognitive Deficits in a COVID-19 Hospitalised Cohort. *EclinicalMedicine* **2022**, *47*, 101417. [[CrossRef](#)]
70. Gaetani, L.; Blennow, K.; Calabresi, P.; Di Filippo, M.; Parnetti, L.; Zetterberg, H. Neurofilament Light Chain as a Biomarker in Neurological Disorders. *J. Neurol. Neurosurg. Psychiatry* **2019**, *90*, 870–881. [[CrossRef](#)]
71. Lin, Y.-S.; Lee, W.-J.; Wang, S.-J.; Fuh, J.-L. Levels of Plasma Neurofilament Light Chain and Cognitive Function in Patients with Alzheimer or Parkinson Disease. *Sci. Rep.* **2018**, *8*, 17368. [[CrossRef](#)] [[PubMed](#)]
72. Romanic, A.M.; White, R.F.; Arleth, A.J.; Ohlstein, E.H.; Barone, F.C. Matrix Metalloproteinase Expression Increases after Cerebral Focal Ischemia in Rats: Inhibition of Matrix Metalloproteinase-9 Reduces Infarct Size. *Stroke* **1998**, *29*, 1020–1030. [[CrossRef](#)] [[PubMed](#)]
73. Rosenberg, G.A. Matrix Metalloproteinases in Neuroinflammation. *Glia* **2002**, *39*, 279–291. [[CrossRef](#)] [[PubMed](#)]
74. Gidday, J.M.; Gasche, Y.G.; Copin, J.-C.; Shah, A.R.; Perez, R.S.; Shapiro, S.D.; Chan, P.H.; Park, T.S. Leukocyte-Derived Matrix Metalloproteinase-9 Mediates Blood-Brain Barrier Breakdown and Is Proinflammatory after Transient Focal Cerebral Ischemia. *Am. J. Physiol. Heart Circ. Physiol.* **2005**, *289*, H558–H568. [[CrossRef](#)] [[PubMed](#)]
75. Planas, A.M.; Solé, S.; Justicia, C. Expression and Activation of Matrix Metalloproteinase-2 and -9 in Rat Brain after Transient Focal Cerebral Ischemia. *Neurobiol. Dis.* **2001**, *8*, 834–846. [[CrossRef](#)]
76. Le, N.D.; Muri, L.; Grandgirard, D.; Kuhle, J.; Leppert, D.; Leib, S.L. Evaluation of Neurofilament Light Chain in the Cerebrospinal Fluid and Blood as a Biomarker for Neuronal Damage in Experimental Pneumococcal Meningitis. *J. Neuroinflamm.* **2020**, *17*, 293. [[CrossRef](#)]
77. Vecil, G.G.; Larsen, P.H.; Corley, S.M.; Herx, L.M.; Besson, A.; Goodyer, C.G.; Yong, V.W. Interleukin-1 Is a Key Regulator of Matrix Metalloproteinase-9 Expression in Human Neurons in Culture and Following Mouse Brain Trauma in Vivo. *J. Neurosci. Res.* **2000**, *61*, 212–224. [[CrossRef](#)]
78. Reinhard, S.M.; Razak, K.; Ethell, I.M. A Delicate Balance: Role of MMP-9 in Brain Development and Pathophysiology of Neurodevelopmental Disorders. *Front. Cell. Neurosci.* **2015**, *9*, 280. [[CrossRef](#)]
79. Sellner, J.; Leib, S.L. In Bacterial Meningitis Cortical Brain Damage Is Associated with Changes in Parenchymal MMP-9/TIMP-1 Ratio and Increased Collagen Type IV Degradation. *Neurobiol. Dis.* **2006**, *21*, 647–656. [[CrossRef](#)] [[PubMed](#)]
80. Muri, L.; Leppert, D.; Grandgirard, D.; Leib, S.L. MMPs and ADAMs in Neurological Infectious Diseases and Multiple Sclerosis. *Cell Mol. Life Sci.* **2019**, *76*, 3097–3116. [[CrossRef](#)]
81. Schönbeck, U.; Mach, F.; Libby, P. Generation of Biologically Active IL-1 Beta by Matrix Metalloproteinases: A Novel Caspase-1-Independent Pathway of IL-1 Beta Processing. *J. Immunol.* **1998**, *161*, 3340–3346. [[PubMed](#)]
82. Anthony, D.C.; Miller, K.M.; Fearn, S.; Townsend, M.J.; Opdenakker, G.; Wells, G.M.; Clements, J.M.; Chandler, S.; Gearing, A.J.; Perry, V.H. Matrix Metalloproteinase Expression in an Experimentally-Induced DTH Model of Multiple Sclerosis in the Rat CNS. *J. Neuroimmunol.* **1998**, *87*, 62–72. [[CrossRef](#)]
83. Leppert, D.; Leib, S.L.; Grygar, C.; Miller, K.M.; Schaad, U.B.; Holländer, G.A. Matrix Metalloproteinase (MMP)-8 and MMP-9 in Cerebrospinal Fluid during Bacterial Meningitis: Association with Blood-Brain Barrier Damage and Neurological Sequelae. *Clin. Infect. Dis.* **2000**, *31*, 80–84. [[CrossRef](#)]
84. Nakaji, K.; Ihara, M.; Takahashi, C.; Itohara, S.; Noda, M.; Takahashi, R.; Tomimoto, H. Matrix Metalloproteinase-2 Plays a Critical Role in the Pathogenesis of White Matter Lesions after Chronic Cerebral Hypoperfusion in Rodents. *Stroke* **2006**, *37*, 2816–2823. [[CrossRef](#)]
85. Moseby-Knappe, M.; Mattsson, N.; Nielsen, N.; Zetterberg, H.; Blennow, K.; Dankiewicz, J.; Dragancea, I.; Friberg, H.; Lilja, G.; Insel, P.S.; et al. Serum Neurofilament Light Chain for Prognosis of Outcome After Cardiac Arrest. *JAMA Neurol.* **2019**, *76*, 64–71. [[CrossRef](#)]

86. Mohammadhosayni, M.; Sadat Mohammadi, F.; Ezzatifar, F.; Mahdavi Gorabi, A.; Khosrojerdi, A.; Aslani, S.; Hemmatzadeh, M.; Yazdani, S.; Arabi, M.; Marofi, F.; et al. Matrix Metalloproteinases Are Involved in the Development of Neurological Complications in Patients with Coronavirus Disease 2019. *Int. Immunopharmacol.* **2021**, *100*, 108076. [[CrossRef](#)]
87. Barro, C.; Chitnis, T.; Weiner, H.L. Blood Neurofilament Light: A Critical Review of Its Application to Neurologic Disease. *Ann. Clin. Transl. Neurol.* **2020**, *7*, 2508–2523. [[CrossRef](#)]
88. Kalm, M.; Boström, M.; Sandelius, Å.; Eriksson, Y.; Ek, C.J.; Blennow, K.; Björk-Eriksson, T.; Zetterberg, H. Serum Concentrations of the Axonal Injury Marker Neurofilament Light Protein Are Not Influenced by Blood-Brain Barrier Permeability. *Brain Res.* **2017**, *1668*, 12–19. [[CrossRef](#)]
89. Uher, T.; McComb, M.; Galkin, S.; Srpova, B.; Oechtering, J.; Barro, C.; Tyblova, M.; Bergsland, N.; Krasensky, J.; Dwyer, M.; et al. Neurofilament Levels Are Associated with Blood-Brain Barrier Integrity, Lymphocyte Extravasation, and Risk Factors Following the First Demyelinating Event in Multiple Sclerosis. *Mult. Scler.* **2021**, *27*, 220–231. [[CrossRef](#)]
90. Suo, T.; Liu, X.; Feng, J.; Guo, M.; Hu, W.; Guo, D.; Ullah, H.; Yang, Y.; Zhang, Q.; Wang, X.; et al. DdPCR: A More Accurate Tool for SARS-CoV-2 Detection in Low Viral Load Specimens. *Emerg. Microbes Infect.* **2020**, *9*, 1259–1268. [[CrossRef](#)]
91. Montalvan, V.; Lee, J.; Bueso, T.; De Toledo, J.; Rivas, K. Neurological Manifestations of COVID-19 and Other Coronavirus Infections: A Systematic Review. *Clin. Neurol. Neurosurg.* **2020**, *194*, 105921. [[CrossRef](#)] [[PubMed](#)]
92. Ramani, A.; Müller, L.; Ostermann, P.N.; Gabriel, E.; Abida-Islam, P.; Müller-Schiffmann, A.; Mariappan, A.; Goureau, O.; Gruell, H.; Walker, A.; et al. SARS-CoV-2 Targets Neurons of 3D Human Brain Organoids. *EMBO J.* **2020**, *39*, e106230. [[CrossRef](#)] [[PubMed](#)]
93. Pellegrini, L.; Albecka, A.; Mallery, D.L.; Kellner, M.J.; Paul, D.; Carter, A.P.; James, L.C.; Lancaster, M.A. SARS-CoV-2 Infects the Brain Choroid Plexus and Disrupts the Blood-CSF Barrier in Human Brain Organoids. *Cell Stem Cell* **2020**, *27*, 951–961. [[CrossRef](#)] [[PubMed](#)]
94. Song, E.; Zhang, C.; Israelow, B.; Lu-Culligan, A.; Prado, A.V.; Skriabine, S.; Lu, P.; Weizman, O.-E.; Liu, F.; Dai, Y.; et al. Neuroinvasion of SARS-CoV-2 in Human and Mouse Brain. *J. Exp. Med.* **2021**, *218*, e20202135. [[CrossRef](#)] [[PubMed](#)]
95. Xia, H.; Lazartigues, E. Angiotensin-Converting Enzyme 2 in the Brain: Properties and Future Directions. *J. Neurochem.* **2008**, *107*, 1482–1494. [[CrossRef](#)]
96. Kumari, P.; Rothan, H.A.; Natekar, J.P.; Stone, S.; Pathak, H.; Strate, P.G.; Arora, K.; Brinton, M.A.; Kumar, M. Neuroinvasion and Encephalitis Following Intranasal Inoculation of SARS-CoV-2 in K18-HACE2 Mice. *Viruses* **2021**, *13*, 132. [[CrossRef](#)]
97. Carossino, M.; Montanaro, P.; O'Connell, A.; Kenney, D.; Gertje, H.; Grosz, K.; Ericsson, M.; Huber, B.R.; Subramaniam, S.; Kirkland, T.A.; et al. Fatal Neuroinvasion and SARS-CoV-2 Tropism in K18-HACE2 Mice Is Partially Independent on HACE2 Expression. *bioRxiv* **2021**, *14*, 535. [[CrossRef](#)]